Acoustic wave propagation in a one-dimensional layered system

Pi-Gang Luan and Zhen Ye
Wave Phenomena Laboratory, Department of Physics, National Central University, Chung-li 32054, Taiwan
(Received 12 October 2000; revised manuscript received 1 March 2001; published 25 May 2001)

Propagation of acoustic waves in a one-dimensional water duct containing many air filled blocks is studied by the transfer matrix formalism. Energy distribution and interface vibration of the air blocks are computed. For periodic arrangement, band structure is calculated analytically, whereas the Lyapunov exponent and its variance are computed numerically for random situations. A distinct collective behavior for localized waves is found. The results are also compared with optical situations.

DOI: 10.1103/PhysRevE.63.066611 PACS number(s): 43.20.+g, 71.55.Jv

I. INTRODUCTION

Propagation of waves in periodic and disordered media has been and continues to be an interesting subject for physicists [1–16]. When propagating in media with inhomogeneities, waves are subject to multiple scattering, which leads to many peculiar phenomena such as band structures in periodic media and wave localization in random media [17–24].

The propagation of waves in one-dimensional (1D) systems has attracted particular interest from scientists because in higher dimensions the interaction between waves and scatterers is so complicated that the theoretical computation is rather involved and most solutions require a series of approximations that are not always justified, making it difficult to relate theoretical predictions to experimental observations. Yet wave localization in 1D poses a more manageable problem that can be tackled in an exact manner by the transfer matrix method [3–9,15]. Moreover, results from 1D can provide insight to the problem of wave localization in general and are suitable for testing various ideas. Indeed, over the past decades considerable progress has been made in understanding the localization behavior in 1D disordered systems [3–9,15]. However, a number of important issues remained untouched. These issues include, for example, how waves are localized inside the media and whether there is a distinct feature for wave localization that would allow to differentiate the localization from residual absorption effect without ambiguity [13,14]. Results from the statistical analysis of the scaling behavior in 1D random media are not conclusive. Another question could be whether the localized state is a phase state that would accommodate a more systematic interpretation [25]. All these motivate us to consider wave propagation in 1D media further, with emphasis on the acoustic wave propagation.

In this paper we study the problem of acoustic wave propagation in a one-dimensional water duct containing many air blocks either regularly or randomly, but on average regularly distributed inside the duct. There are a few advantages in using such a 1D liquid system and it has been a popular model for underwater acoustic problems (e.g., [7]). First, the system is simple enough to warrant the accurate extraction of many significant results. Second, the acoustic impedance between air and water is so significant that a study of strong acoustic scattering is made possible. Third, this example is complicated enough to illustrate many important characteristics of wave localization in a 1D system. Fourth, we think that given the simplicity in the system, an experimental observation is quite possible. Last but not the least, the planar bubble system has been an integral part of the theoretical exploration of underwater gas bubbles [26]. In this article, the frequency band structures and wave transmission are computed numerically. We show that while our results affirm the previous claim that all waves are localized inside a 1D medium with any amount of disorder, there are, however, a few distinctive features in our results. Among them, in contrast to the optical case [15], there is no universal scaling behavior in the present system. In addition, when waves are localized, a collective behavior of the system emerges. We will also show the energy distribution in the water duct.

This paper is organized as follows. In the next section we explain the model employed, discuss the transfer matrix method, and derive relevant formulas. In Sec. III numerical results and discussions are given. We then summarize the paper in Sec. IV.

II. MODEL AND METHOD

A. System setup

We study a system consisting of air blocks inside a water duct. This system is chosen because air filled blocks are strong acoustic scatterers. This can be seen as follows. The scattering is largely controlled by the acoustic impedance, which is defined as ρc, with ρ and c being the mass density of the medium and the acoustic phase speed, respectively. The acoustic impedance ratio between water and air is about 3500. This large contrast leads to strong scattering, making the system of air blocks in water an ideal candidate for the study of acoustic scattering.

The 1D acoustic system we consider is illustrated by Fig. 1. Assume that N air blocks of thickness a_j $(j=1,\ldots,N)$ are placed regularly or randomly in a water duct with length L measured from the left boundary (LB) of the duct. The distance from the LB to the left interface of the first air block is D. For simplicity while without compromising generality, in later numerical computation we set the thickness of each air block to the same value a. The air fraction is clearly $\beta = Na/L$, the average distance between two adjacent air or water blocks is $\langle d\rangle = L/N = a/\beta$, and the average thickness of water blocks is $\langle b\rangle = (D+\Sigma_{j=1}^{N-1} b_j)/N$. The degree of ran-

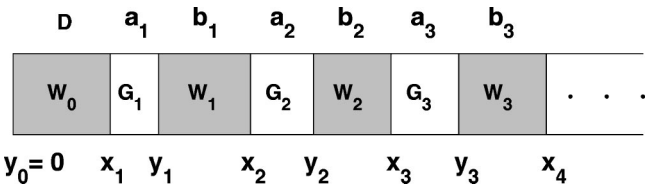

FIG. 1. Regular and random arrangements of air blocks in the duct. The symbols $\mathbf{G}_j$, $\mathbf{W}_j$ denote the air and water layers; a_j and b_j represent their thicknesses; the jth air block and the water separated by the jth and $(j+1)$th air blocks, denoted as the jth water block, is regarded as one unit and is labeled as the jth unit; therefore $d_j = a_j + b_j$ represents the thickness of the jth unit. $x_j = D + \Sigma_{l=1}^{j-1} d_l$ and $y_j = x_j + a_j$ represent the positions of air-water and water-air interfaces. For regular arrangement $a_j = a$, $b_j = b$, $d_j = d = a + b$ and $x_j = D + (j-1)d$, $y_j = x_j + a$.

domness for the system is controlled by a parameter Δ in such a way that the thickness of the jth water block is $b_j = \langle b \rangle (1+\delta_j)$, δ_j being a random number within the interval $[-\Delta, \Delta]$; the regular case corresponds to $\Delta = 0$. An acoustic source placed at the LB generates monochromatic waves with an oscillation $v(t) = v e^{-i\omega t}$. Transmitted waves propagate through the N air blocks and travel to the right infinity. In order to avoid unnecessary confusion, possible effects from surface tension, viscosity, or any absorption are neglected.

For convenience, we use the dimensionless quantity $k\langle b \rangle$ to measure the frequency, where $k = \omega/c$ is the wave number in water blocks. Similarly, k_g represents the wave number in air blocks. We also define the following parameters for later use

$$g = \frac{\rho_g}{\rho}, \quad h = \frac{c_g}{c} = \frac{k}{k_g}, \quad q^2 = gh, \quad \eta = \ln q. \tag{1}$$

B. Wave propagation and state vector

The problem of wave propagation is readily studied by the transfer matrix method [4]. In the following, we will only briefly show the approach and present the relevant results. Dropping the time factor $e^{-i\omega t}$, the pressure wave $p(x)$ within any layer (air block or water block) is the plane wave

$$p(x) = A e^{ikx} + B e^{-ikx}, \tag{2}$$

where Ae^{ikx} represents the wave transmitted away from the source to the right, Be^{-ikx} is the wave reflected towards the source and k refers to the wave number in the corresponding medium. The velocity field u, which describes the oscillation of the medium, is written as

$$u(x) = \frac{1}{i\omega\rho} p'(x) = \frac{1}{\rho c} [A e^{ikx} - B e^{-ikx}], \tag{3}$$

where ρ refers to the mass density of the corresponding layer. By invoking the continuity conditions of pressure and velocity fields at the interfaces that separate water and air, and imposing the boundary conditions at two ends of the system, the problem can be solved.

To proceed we define a state vector in the corresponding layer as

$$\mathbf{S}(x) \equiv \begin{pmatrix} S^1(x) \\ S^2(x) \end{pmatrix} = \begin{pmatrix} A(x) \\ B(x) \end{pmatrix} = \begin{pmatrix} Ae^{ikx} \\ Be^{-ikx} \end{pmatrix}, \tag{4}$$

then $p(x)$ and $u(x)$ are expressed as linear combinations of the two components of $\mathbf{S}(x)$. In what follows we denote the state vector in the jth air block as $\mathbf{G}_j(x)$ with two components $G_j^1(x) = G_j^1 e^{ik_g x}$ and $G_j^2(x) = G_j^2 e^{-ik_g x}$, and in the jth water block as $\mathbf{W}_j(x)$ with $W_j^1(x) = W_j^1 e^{ikx}$ and $W_j^2(x) = W_j^2 e^{-ikx}$. Invoking the continuity condition of p and u at the water-air interfaces that are located at x_j (see Fig. 1), we find

$$\mathbf{W}_{j-1}(x_j) = J \mathbf{G}_j(x_j), \quad \mathbf{G}_j(y_j) = J^{-1} \mathbf{W}_j(y_j),$$

with

$$J = q^{-1} \begin{pmatrix} \cosh\eta & \sinh\eta \\ \sinh\eta & \cosh\eta \end{pmatrix}. \tag{5}$$

For wave propagation in the jth air or water layer, we have

$$\mathbf{G}_j(x_j) = U_g(a_j) \mathbf{G}_j(y_j), \tag{6}$$

with

$$U_g(a_j) = \begin{pmatrix} e^{-ik_g a_j} & 0 \\ 0 & e^{ik_g a_j} \end{pmatrix},$$

and

$$\mathbf{W}_j(y_j) = U(b_j) \mathbf{W}_j(x_{j+1}), \tag{7}$$

with

$$U(b_j) = \begin{pmatrix} e^{-ikb_j} & 0 \\ 0 & e^{ikb_j} \end{pmatrix}.$$

From these results the transfer matrix M_j for the jth unit is

$$M_j = J U_g(a_j) J^{-1} U(b_j) \tag{8}$$

and the state vectors in water blocks satisfy

$$\mathbf{W}_{j-1}(x_j) = M_j \mathbf{W}_j(x_{j+1}). \tag{9}$$

Therefore any two state vectors of the water blocks are connected as

$$\mathbf{W}_{j_1-1}(x_{j_1}) = M_{j_1, j_2} \mathbf{W}_{j_2}(x_{j_2+1}), \tag{10}$$

where

$$M_{j_1, j_2} = M_{j_1} M_{j_1+1} \cdots M_{j_2}, \quad 1 \leqslant j_1 \leqslant j_2 \leqslant N. \tag{11}$$

From Eqs. (8) and (11) one can easily prove that all M_{j_1, j_2} are unimodular matrices, a result of energy conservation. Define

$$M_{1,N} \equiv \mathcal{M} = \begin{pmatrix} \mathcal{M}_{11} & \mathcal{M}_{12} \\ \mathcal{M}_{21} & \mathcal{M}_{22} \end{pmatrix}, \tag{12}$$

then a simple reduction leads to

$$\mathcal{M}_{21} = \mathcal{M}_{12}^*, \quad \mathcal{M}_{22} = \mathcal{M}_{11}^*. \tag{13}$$

It is clear that the transfer matrix $M_{1,N}$ connects the first water block and the last water block.

Imposing the boundary conditions at the LB

$$v = \frac{1}{\rho c}[W_0^1 - W_0^2], \tag{14}$$

and

$$W_N^2 = 0 \tag{15}$$

at the rightmost boundary, we obtain

$$\mathbf{W}_0(x_1) = \frac{\rho c v}{\mathcal{M}_{11} e^{-ikD} - \mathcal{M}_{12}^* e^{ikD}} \begin{pmatrix} \mathcal{M}_{11} \\ \mathcal{M}_{12}^* \end{pmatrix}. \tag{16}$$

By substituting Eq. (16) into Eq. (10) and letting $j_1 = 1$ and $j_2 = j$, the state vector $\mathbf{W}_j$ and both p and u in the jth layer are determined.

C. Lyapunov exponent

Waves propagating through N air blocks will be scattered many times before they go out. The total transmission and reflection rates can be obtained from the scattering matrix M^s,

$$M^s = \begin{pmatrix} 1/t & r^*/t^* \\ r/t & 1/t^* \end{pmatrix},$$

where t and r are transmission and reflection coefficients, and $T = |t|^2$ and $R = |r|^2$ define the transmission and reflection rates. Based on the previous discussion

$$M^s = M_{1,N} = \mathcal{M} \tag{17}$$

and

$$T_N = \frac{1}{|\mathcal{M}_{11}|^2}, \quad R_N = \frac{|\mathcal{M}_{12}|^2}{|\mathcal{M}_{11}|^2}. \tag{18}$$

Note that in Eq. (18) the relation $T_N + R_N = 1$ is satisfied, which is a consequence of energy conservation since the system we considered does not absorb any energy.

It is well known that in a random medium waves are always localized in space and the localization is characterized by the Lyapunov exponent (LE) γ. The Lyapunov exponent is defined as

$$\gamma = \lim_{N \to \infty} \langle \gamma_N \rangle, \tag{19}$$

with

$$\gamma_N \equiv \frac{1}{2N} \ln\left(\frac{1}{T_N}\right). \tag{20}$$

The fluctuation or variance of γ defined by

$$\mathrm{var}(\gamma) = \lim_{N \to \infty} (\langle \gamma_N^2 \rangle - \langle \gamma_N \rangle^2) \tag{21}$$

is a quantity that, as will be shown below, gives important information about the system.

D. Energy distribution and phase vector

The time averaged energy density $\mathcal{E}(x)$ at x are defined by

$$\mathcal{E}_m(x) = \frac{\rho_m}{4}\left[|u_m|^2 + \frac{|p_m|^2}{\rho_m^2 c_m^2} \right]. \tag{22}$$

By direct calculations we find that the energy density in our 1D system is piecewise constant and hence we can suppress the redundant variable x. Energy density in the jth water block $\mathcal{E}_j^w$ and in the jth air block $\mathcal{E}_j^g$ are given by

$$\mathcal{E}_j^w = \frac{1}{2\rho c^2}[\,|W_j^1|^2 + |W_j^2|^2] \tag{23}$$

and

$$\mathcal{E}_j^g = \frac{1}{2\rho_g c_g^2}[|G_j^1|^2 + |G_j^2|^2]. \tag{24}$$

When waves propagate through media alternated with different material compositions, multiple scattering of waves is established by an infinite recursive pattern of rescattering. Writing $p(x) = A(x) e^{i\theta(x)}$, with $A(x) = |p(x)|$ and θ being the amplitude and phase, respectively, the energy flow $\mathcal{J} \sim \mathrm{Re}[i(p^*(x)\partial_x p(x)]$ becomes $\mathcal{J} \sim A^2 \partial_x \theta$. Obviously, the energy flow will come to a complete halt and the waves are localized in space when A is not equal to zero but phase θ is constant at least by domains.

From these observations, we propose to use the phase behavior of waves to characterize the wave localization. Expressing $p(x)$ and $u(x)$ as

$$p(x) \equiv A_p(x) e^{i\theta_p(x)} \tag{25}$$

and

$$u(x) \equiv A_u(x) e^{i\theta_u(x)}, \tag{26}$$

we construct two unit phase vectors as

$$\vec{v}_p \equiv \hat{e}_x \cos\theta_p + \hat{e}_y \sin\theta_p \tag{27}$$

and

$$\vec{v}_u \equiv \hat{e}_x \cos\theta_u + \hat{e}_y \sin\theta_u. \tag{28}$$

Physically, these phase vectors represent the oscillation behavior of the system. We can plot the phase vectors in a two-dimensional plane.

E. Band structure

According to the Bloch theorem, the eigenmodes of wave field p and velocity field u in an infinite periodic medium can be written as

$$p(x)=\xi(x)e^{iKx}, \quad u(x)=\zeta(x)e^{iKx} \tag{29}$$

where $\xi(x)$ and $\zeta(x)$ are periodic functions satisfying $\xi(x+d)=\xi(x)$, $\zeta(x+d)=\zeta(x)$ and K is the usual Bloch wave number.

Equation (29) implies

$$e^{-iKd}\mathbf{W}_j(x_j+d)=\mathbf{W}_{j-1}(x_j)=M\mathbf{W}_j(x_j+d), \tag{30}$$

where $M=M_j$ is the transfer matrix for a single unit (period) and e^{-iKd} is the eigenvalue of matrix M. The dispersion relation is given by

$$\cos Kd=\cos k_g a\cos kb-\cosh 2\eta\sin k_g a\sin kb. \tag{31}$$

The frequency ranges within which real solutions for K can be deduced define the pass bands, while the ranges rending the complex solutions for K determine the stop bands (band gaps).

III. NUMERICAL RESULTS AND DISCUSSION

A. Ordered cases

In the ordered case, the interference of multiply scattered waves leads to frequency band structures. For frequencies located in pass bands, waves propagate through the whole system, while for frequencies within a band gap, waves are evanescent.

In Fig. 2(a), $\cos Kd$ versus kb/π from Eq. (31) are displayed for $\beta=10^{-4}$ (solid curve) and $\beta=3\times10^{-5}$ (broken curve). The segments of curves between $\cos Kd=\pm1$ (the gray region) give real solutions of Kd and correspond to pass bands, whereas those outside of the gray region correspond to forbidden bands. Figure 2(b) shows the relation between the pass/forbidden bands and the fraction of air blocks, β. It is seen that for $\beta>10^{-3}$ and $kb>3\pi$, the pass bands almost vanish. The band structures for various bands are shown in Figs. 2(c) and 2(d). We see that as the volume fraction β increases, the width of the pass bands decrease and the width of band gaps become larger. As expected from the earlier discussion, the fact that air blocks are very strong acoustic scatterers in water leads to very wide band gaps and narrow pass bands shown in Figs. 2(c) and 2(d).

Figure 3 shows the energy density distribution along the duct for $N=100$ air blocks. In parts (a), (b), (c), and (d), of Fig. 3(A), the energy density in water blocks is shown, whereas in parts (a), (b), (c), and (d) of Fig. 3(B), the energy density in the air blocks is displayed. In the computation, the air fraction is taken as $\beta=10^{-4}$. We find that for frequencies located in the pass bands, the energy density varies periodically along the traveling path. For frequencies within the frequency gaps, the energy is trapped near the acoustic source, and the energy density decays about exponentially along the path. Meanwhile, the energy flow is calculated to be close to zero.

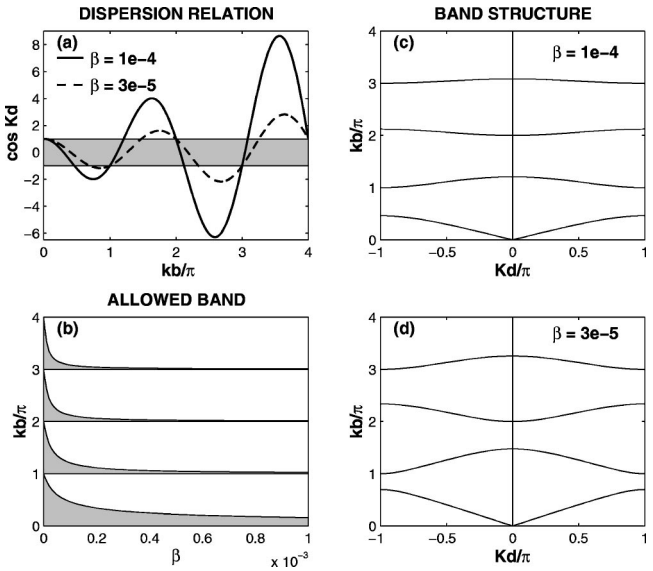

FIG. 2. Various properties of periodic system. (a) Dispersion relations for air fractions $\beta=10^{-4}$ (solid line) and $\beta=3\times10^{-5}$ (broken line). Segments of curves inside the gray region bounded by $\cos Kd=\pm1$ correspond to the propagating waves (allowed bands), whereas those outside of the gray region represent evanescent waves (band gaps). (b) Allowed bands (gray regions) versus air fraction β. (c) Band structure for $\beta=10^{-4}$. (d) Band structure for $\beta=3\times10^{-5}$. Here K is the Bloch wave number, d is the lattice spacing.

We now look at the oscillation behavior of the blocks. As discussed above, zero energy flow leads to a phase coherence behavior of the medium. For the purpose we consider the behavior of the phase vectors $\vec{v}_p$ and $\vec{v}_u$ defined in Eqs. (27) and (28). Typical results of phase behavior are shown in Fig. 4. For further convenience, only the phase vectors at the interfaces between air and water are shown. Symbols p^L, p^R, u^L, u^R appearing in Fig. 4 denote, respectively, the phase vectors for the pressure and the velocity fields on the left and right side of the air blocks. We set the vibration phase of the LB to 1. First we discuss the cases shown in Figs. 4(a) and 4(b). The frequencies in Figs. 4(a) and 4(b) are chosen from the first pass band. The phase vectors in these two cases point to various directions along the duct and $\vec{v}_p\cdot\vec{v}_u\neq0$, resulting in a nonzero energy flow. The waves are extended in the system. In Figs. 4(c) and 4(d), the frequencies are chosen from the first band gap in which waves are evanescent as shown in Fig. 3. In this case, all the phase vectors of the pressure field are pointing to either $\pi/2$ or $-\pi/2$, and are perpendicular to the phase vectors of the velocity field. The pressure at the two sides of any air block is almost in phase. Different from the higher-dimensional cases in which all phase vectors of localized fields point to the same direction [11,16], the present phase vectors are constant only by domains. The velocity field in neighboring domains oscillate with a phase difference π. At the far end of the sample,

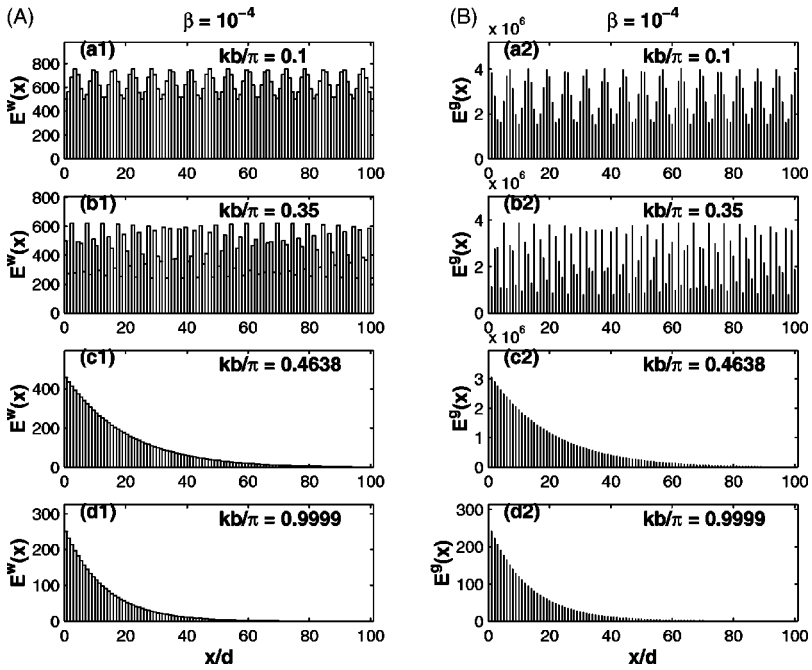

FIG. 3. Energy density distributions along the duct at four different frequencies: $kb/\pi=0.02$, 0.35, 0.4638, 0.9999. (A) Parts (a)–(d): Energy density in water blocks. (B) Parts (a)–(d): Energy density in air blocks. Number of air blocks $N=100$ and air fraction $\beta=10^{-4}$. Vibration velocity of the LB is chosen as $v=1$ m/s.

however, the phase vectors become gradually disoriented, implying that the energy can leak out only at the boundary due to the finite sample size. We note here that such a phase ordering not only exists for the boundaries of the air blocks, but also appears inside the whole medium.

B. Disordered situations

Unlike in the ordered case for which waves can propagate through all air blocks if the frequency is located in the pass band, in a disordered 1D system waves are always localized. In this section, we study numerically acoustic propagation in the disordered case.

Figure 5(a) presents the typical results of the transmission rate as a function of $k\langle b\rangle$ for various β at a given randomness. At frequencies for which the wavelength is smaller than the averaged distance between air blocks, the transmission is significantly reduced by increasing air fraction.

Figure 5(b) illustrates the effect of the randomness Δ on transmission for a given air fraction. For comparison, the transmission in the corresponding regular array ($\Delta=0$) is also plotted. The gaps are located between $k\langle b\rangle/\pi=0.4638$ and 1, 1.21 and 2, 2.128 and 3, and so on. We find that for frequencies located inside the band gaps of the corresponding periodic array, the disorder-induced localization effect competes yet reduces the band gap effect. To characterize wave localization in this case, both the band gap and the disorder effects should be considered, supporting the two-parameter scaling theory [15]. However, increasing disorder tends to smear out the band structures. When exceeding a certain amount, the effect from the disorder suppresses the band gap effect completely, and there is no distinction between the localization at frequencies within and outside the band gaps.

Figure 5 shows that the localization behavior depends crucially on whether the wavelength λ is greater than the average distance between air blocks. When $\langle b\rangle/\lambda$ is less than 1/4, the localization effect is weak. We also observe that with the added disorder, the transmission is enhanced in the middle of the gaps. Similar enhancement due to disorder has also been reported recently [9]. Differing from [9], however, the transmission at frequencies within the gaps of the corresponding periodic arrays in the present system is not always enhanced by disorder. Instead the transmission is reduced further by the disorder near the band edges.

To further explore the transmission property, we calculate the Lyapunov exponent γ and its variance var(γ) according to Eqs. (19) and (21). The sample size is chosen in such a way that it is much larger than the localization length and the ensemble average is carried out over 2000 random configurations. Figure 6 presents the results for the LE and its variance as a function of $k\langle b\rangle/\pi$ for various random configurations. As expected, when the randomness is small the LE mimics the band structures and the variance of the LE inside the gaps is small. In contrast to the optical case [15], there

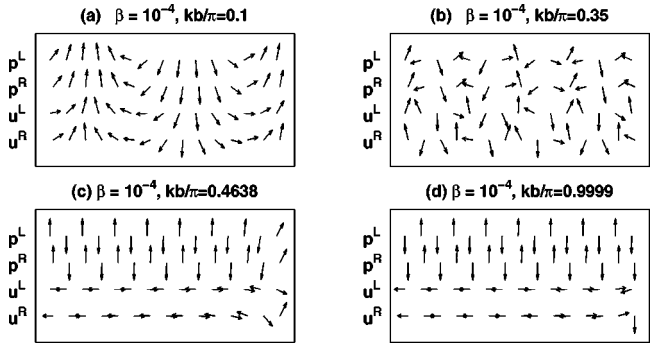

FIG. 4. Phase vectors at air block boundaries. Total number of air blocks is $N=15$ and the air fraction is $\beta=10^{-4}$. Four frequencies are chosen according to Fig. 3, that is, $kb/\pi=0.02$ and 0.35 in the first allow band, and $kb/\pi=0.4638$ and 0.9999 in the first gap. In the diagrams, the small arrows are used to represent the phase vectors.

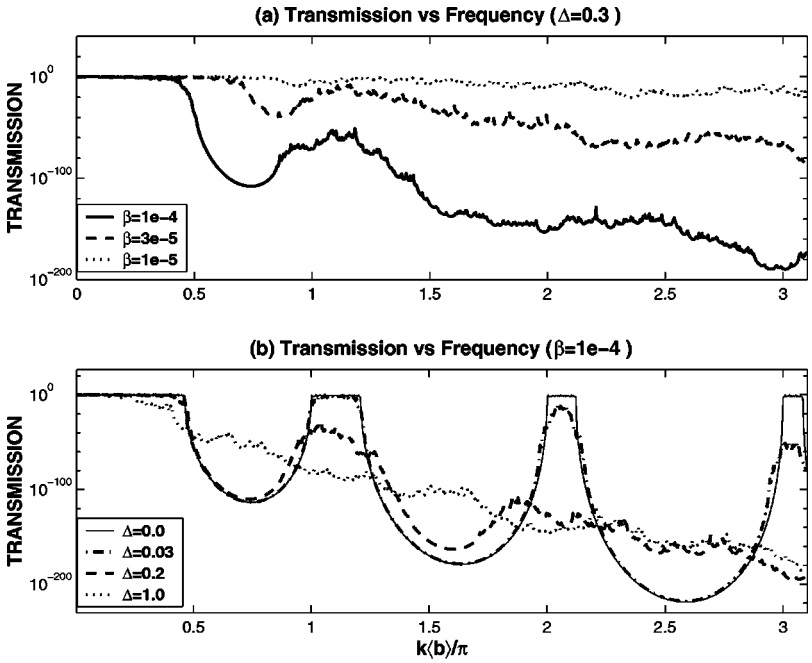

FIG. 5. Transmission versus $k\langle b\rangle/\pi$ for various air fractions at $\Delta=0.3$ (a) and different disorders (b). The number of the air blocks is 100.

are no double maxima for the variance inside the gap. Rather, the double peaks appear in the allowed bands when the system is disordered. The double peak feature is more prominent in the low frequency bands. When the randomness exceeds a certain value, however, the double peaks emerge. Higher the frequency, lower is the critical value. For example, the double peaks are still visible in the first allowed band [cf. Fig. 6(b)], while there is only one peak inside the higher pass bands. Meanwhile, the increasing disorder reduces the band gap effect and smears out the oscillation in the LE, in accordance with Fig. 6. We also plot the LE versus its variance in Fig. 6. When randomness is weak, several branches appear in the LE-variance relation. The frequency range of a branch covers a pass band. In the optical case, the frequency range of a branch covers a gap instead [15]. A prominent feature in the present system is that when the double peaks in the variance are destroyed, the minima of the LE correspond to the maxima of its variance. This is different from the optical case [15].

With increasing disorder, we do not observe the genuine linear dependence between the LE and its variance, as expected from the single-parameter scaling theory [24], indicating that the single-parameter scaling law may not be applicable in the present system.

Equations (23) and (24) provide the formulas for studying energy distributions in any situation. As discussed in the regular case, when the wave is localized, a kind of ordering of the phase vectors appears. From the alignment pattern of phase vectors we can know whether waves inside the system are localized. For air fraction $\beta=10^{-4}$, three different cases with different $k\langle b\rangle/\pi$, Δ, and N are shown in Figs. 7, 8, and 9. To isolate the localization effect from the band gap effects,

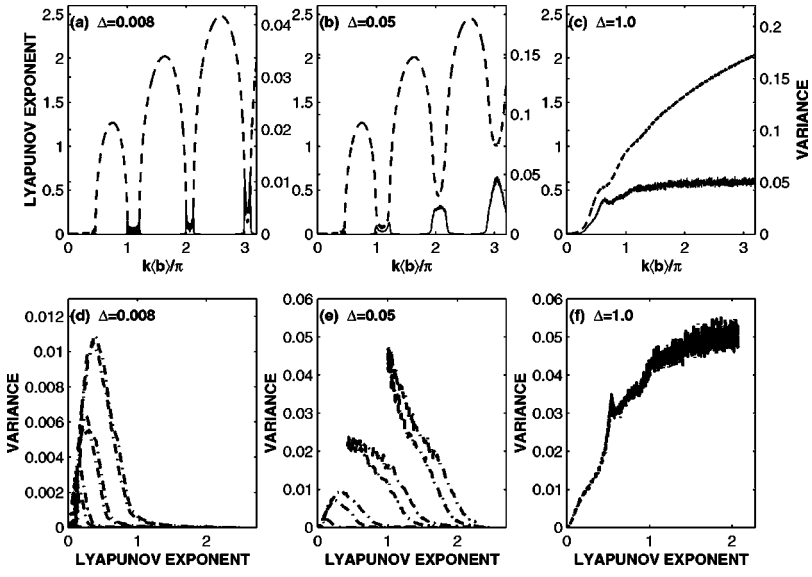

FIG. 6. (a), (b), and (c) show the Lyapunov exponent (LE) in broken lines and its variance in solid lines as a function of $k\langle b\rangle/\pi$ for three random situations. (d), (e), and (f) present the plots of the exponent versus its variance in the three random cases. Here $\beta=10^{-4}$.

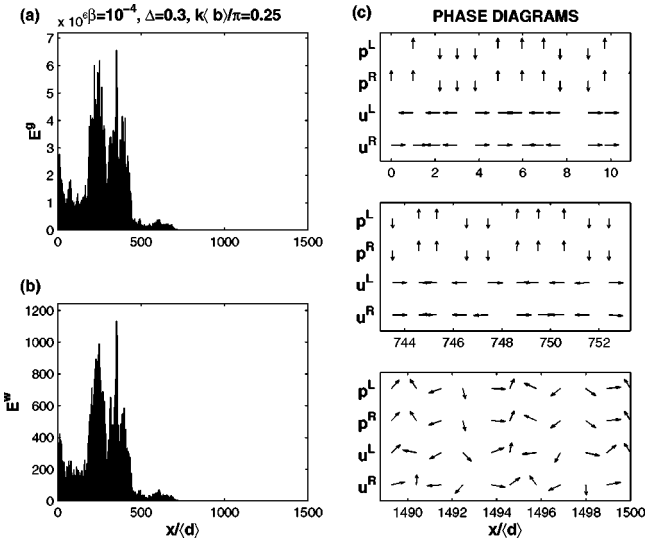

FIG. 7. Energy density distributions along the duct in air blocks (a) and in water blocks (b). Phase vectors at the interfaces for three spatial ranges of the medium are illustrated in (c). The unit of energy density is J/m^3, air fraction $\beta=10^{-4}$, $k\langle b\rangle/\pi=0.25$, $\Delta=0.3$, $N=1500$. Vibration velocity of the LB is chosen as $v=1$ m/s.

we choose the two frequencies located in the first allowed band: one is in the middle of the band and the other is near the lower band edge.

First, we note that the energy density is constant in each individual block. This is a special feature of 1D classical systems and can be verified by a deduction from Eqs. (23) and (24). From these figures, we observe that when the sample size is sufficiently large, waves are always localized

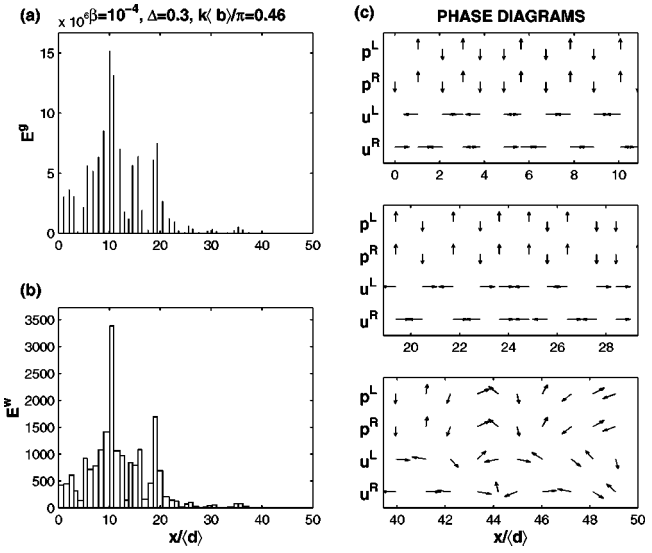

FIG. 8. Energy density distributions along the duct in air blocks (a) and in water blocks (b). Phase vectors at the interfaces for three spatial ranges of the medium are illustrated in (c). The unit of energy density is J/m^3, air fraction $\beta=10^{-4}$, $k\langle b\rangle/\pi=0.46$, $\Delta=0.3$, $N=50$. Vibration velocity of the LB is chosen as $v=1$ m/s.

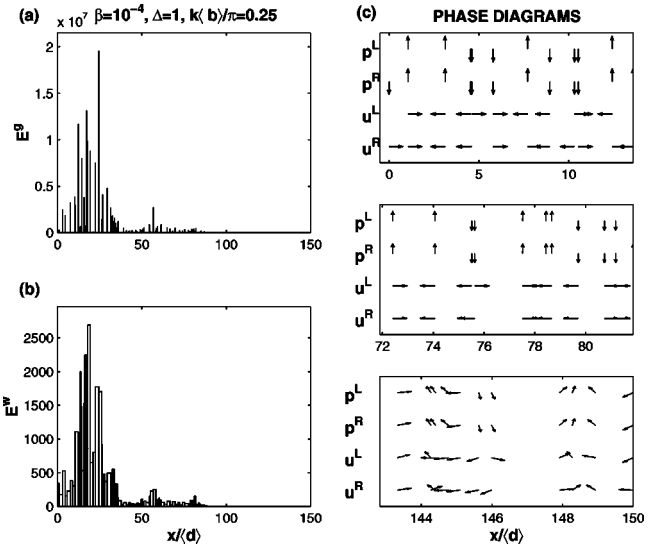

FIG. 9. Energy density distributions along the duct in air blocks (a) and in water blocks (b). Phase vectors at the interfaces for three spatial ranges of the medium are illustrated in (c). The unit of energy density is J/m^3, air fraction $\beta=10^{-4}$, $k\langle b\rangle/\pi=0.25$, $\Delta=1$, $N=150$. Vibration velocity of the LB is chosen as $v=1$ m/s.

for any given amount of randomness. When localized, the waves are trapped inside the medium, but not necessarily confined at the site of the source, unless the band gap effect is dominant. The energy distribution does not follow an exponential decay along the path. This differs from situations in higher dimensions [10,16]. It is also shown that the energy stored in the medium can be tremendous.

These figures also show that for low frequencies and when the randomness is small, to trap the waves a large number of air blocks is needed. Like in the regular cases, when waves are localized, the coherent behavior of the medium appears, and the phases are constant by domains. The phase vector domains are sensitive to the arrangement of the air blocks. Moreover, when localization is evident, increasing the sample size by adding more air blocks to the far end of the system will not change the patterns of the energy distribution and phase vectors. Therefore the energy localization and the phase coherence behavior are not caused by the boundary effect.

Figure 7 shows the energy distribution inside the medium. Here we choose $k\langle b\rangle/\pi=0.25$, which is inside the first pass band. We see that the energies are localized in both air and water blocks. However, unlike in the regular cases, the energy does not always decay exponentially along the path. In Fig. 8 we use the same parameters as in Fig. 7 except that we choose $k\langle b\rangle/\pi=0.46$, which is very close to the gap edge 0.4638. We see now that waves can be very easily trapped by using only $N=50$ air blocks. In Fig. 9 we choose $k\langle b\rangle/\pi=0.25$ as used in Fig. 7 but increase the randomness to $\Delta=1$, waves are trapped by $N=150$ air blocks, fewer than in the case of Fig. 7.

IV. CONCLUDING REMARKS

In this paper we studied the propagation of acoustic waves in 1D layered system consisting of air and water

blocks. For periodically placed air blocks, the band structures were studied and were shown to have large band gaps. For the case of randomly placed air blocks, the transmission, Lyapunov exponent and its variance, energy distribution and medium vibration were studied. The results pointed out that waves are always confined in a finite spatial region. The disorder leads to a significant energy storage in the system. It is also indicated that the wave localization is related to a collective behavior of the system in the presence of multiple scattering, also observed for higher dimensions [11,16]. The appearance of such a collective phenomenon may be regarded as an indication of a kind of classical Goldstone modes in the context of the field theory [25].

ACKNOWLEDGMENT

The work received support from the National Science Council (Grant Nos. NSC89-2611-M008-002 and NSC89-2112-M008-008).

[1] *Scattering and Localization of Classical Waves in Random Media*, edited by P. Sheng (World Scientific, Singapore, 1990).
[2] A. Ishimaru, *Wave Propagation and Scattering in Random Media* (Academic, New York, 1978).
[3] C. H. Hodges and J. Woodhouse, J. Acoust. Soc. Am. **74**, 894 (1983).
[4] V. Baluni and J. Willemsen, Phys. Rev. A **31**, 3358 (1985).
[5] H. Matsuda and K. Ishii, Suppl. Prog. Theor. Phys. **45**, 56 (1970).
[6] C. M. Soukoulis, S. Datta, and E. N. Economou, Phys. Rev. B **49**, 3800 (1994).
[7] D. Sornette and O. Legrand, J. Acoust. Soc. Am. **92**, 296 (1992).
[8] A. R. McGurn, K. T. Christensen, F. M. Mueller, and A. A. Maradudin, Phys. Rev. B **47**, 13 120 (1993).
[9] V. D. Freilikher, B. A. Liansky, I. V. Yurkevich, A. A. Maradudin, and A. R. McGurn, Phys. Rev. E **51**, 6301 (1995).
[10] Z. Ye and A. Alvarez, Phys. Rev. Lett. **80**, 3503 (1998).
[11] Z. Ye, H. Hsu, E. Hoskinson, and A. Alvarez, Chin. J. Phys. (Taipei) **37**, 343 (1999).
[12] R. Dalichaouch, J. P. Armstrong, S. Schultz, P. M. Platzman, and S. L. McCall, Nature (London) **354**, 53 (1991).
[13] F. Scheffold, R. Lenke, R. Tweer, and G. Maret, Nature (London) **398**, 206 (1999); D. S. Wiersma, P. Bartolini, A. Lagendjik, and R. Righini, *ibid.* **390**, 671 (1997).
[14] A. A. Chabanov, M. Stoytchev, and A. Z. Genack, Nature (London) **404**, 850 (2000).
[15] Lev I. Deych, D. Zaslavsky, and A. A. Lisyansky, Phys. Rev. Lett. **81**, 5390 (1998).
[16] E. Hoskinson and Z. Ye, Phys. Rev. Lett. **83**, 2734 (1999).
[17] K. M. Leung and Y. Qiu, Phys. Rev. B **48**, 7767 (1993).
[18] E. Yablonovitch, Science **289**, 557 (2000).
[19] M. S. Kushwaha, P. Halevi, and G. Martinez, Phys. Rev. B **49**, 2313 (1994).
[20] E. N. Economou and M. Sigalas, J. Acoust. Soc. Am. **95**, 1734 (1994).
[21] J. V. Sánchez-Pérez, D. Caballero, R. Mártinez-Sala, C. Rubio, J. Sánchez-Dehesa, F. Meseguer, J. Llinares, and F. Gálvez, Phys. Rev. Lett. **80**, 5325 (1998).
[22] M. Torres, F. R. Montero de Espinosa, D. Garcia-Pablos, and N. Garcia, Phys. Rev. Lett. **82**, 3054 (1999).
[23] P. W. Anderson, Phys. Rev. **109**, 1492 (1958).
[24] P. W. Anderson, D. J. Thouless, E. Abrahams, and D. S. Fisher, Phys. Rev. B **22**, 3519 (1980).
[25] H. Umezawa, *Advanced Field Theory* (AIP, New York, 1995).
[26] D. Epstein and J. B. Keller, J. Acoust. Soc. Am. **52**, 975 (1971).